TYPE Ia SNe ALONG REDSHIFT: THE $\mathcal{R}$(Si II) RATIO AND THE EXPANSION VELOCITIES IN INTERMEDIATE-z SUPERNOVAE

G. ALTAVILLA[1], P. RUIZ-LAPUENTE[1,2], A. BALASTEGUI[1], J. MÉNDEZ[1,3], M. IRWIN[4], C. ESPAÑA-BONET[1], R. S. ELLIS[4,5],
G. FOLATELLI[6], A. GOOBAR[6], W. HILLEBRANDT[2], R. M. MCMAHON[4], S. NOBILI[6], V. STANISHEV[6], AND N. A. WALTON[4]

[1] Department of Astronomy, University of Barcelona, Diagonal 647, E-08028 Barcelona, Spain
[2] Max-Planck Institut für Astrophysik, Karl Schwarzschildstrasse 1, D-85741 Garching, Germany
[3] Isaac Newton Group of Telescopes, 38700 Santa Cruz de La Palma, Islas Canarias, Spain
[4] Institute of Astronomy, University of Cambridge, Madingley Road, Cambridge CB3 0HA, UK
[5] California Institute of Technology, Pasadena, CA 91125, USA
[6] Department of Physics, Stockholm University, SE-10691 Stockholm, Sweden

ABSTRACT

We present a study of intermediate-z Type Ia supernovae (SNe Ia) using empirical physical diagrams which permit the investigation of those SNe explosions. This information can be very useful to reduce systematic uncertainties of the Hubble diagram of SNe Ia up to high z. The study of the expansion velocities and the measurement of the ratio $\mathcal{R}$(Si II) allow subtyping of SNe Ia as done in nearby samples. The evolution of this ratio as seen in the diagram $\mathcal{R}$(Si II)–(t) together with $\mathcal{R}$(Si II)$_{max}$ versus $(B-V)_0$ indicates consistency of the properties at intermediate-z compared with the nearby SNe Ia. At intermediate-z, expansion velocities of Ca II and Si II are found similar to those of the nearby sample. This is found in a sample of six SNe Ia in the range $0.033 \leqslant z \leqslant 0.329$ discovered within the *International Time Programme* of SNe Ia for Cosmology and Physics in the spring run of 2002.[7] Two SNe Ia at intermediate-z were of the cool FAINT type, one being an SN1986G-like object highly reddened. The $\mathcal{R}$(Si II) ratio as well as subclassification of the SNe Ia beyond templates help to place SNe Ia in their sequence of brightness and to distinguish between reddened and intrinsically red supernovae. This test can be done with very high z SNe Ia and it will help to reduce systematic uncertainties due to extinction by dust. It should allow to map the high-z sample into the nearby one.

Key words: cosmology: observations – supernovae: general – supernovae: individual (2002li, 2002lj, 2002lk, 2002ln, 2002lo, 2002lp, 2002lq, 2002lr)

Online-only material: color figures

1. INTRODUCTION

The measurements using Type Ia supernovae (SNe Ia) of the expansion rate of the universe led to the discovery of its acceleration (Riess et al. 1998; Perlmutter et al. 1999) and have opened a new field in the identification of the driving force of the accelerated expansion, the so-called dark energy. A large local supernova sample was first studied in the Calan–Tololo survey (Hamuy et al. 1996) and nowadays in a series of campaigns at low redshift by various collaborations. At high-z, the first supernova samples were gathered by the Supernova Cosmology Project (Perlmutter et al. 1999; Knop et al. 2003; Hook et al. 2005; Kowalski et al. 2008) and the High-z SN Team/ESSENCE (Riess et al. 1998; Tonry et al. 2003; Barris et al. 2004; Krisciunas et al. 2005; Clocchiatti et al. 2006; Wood-Vasey et al. 2007). In recent years, the high-z redshift range has been targeted as well by the Supernova Legacy Survey (Astier et al. 2006). The combination of the discoveries made by all these collaborations will provide hundreds of SNe Ia at $z > 0.2$. At very high redshift, the Higher-z Team using the *Hubble Space Telescope* (*HST*) concentrates in the discovery of supernovae at $z > 1$ to better constraint dark energy (Riess et al. 2004, 2007). This is also the target of the latest runs of the Supernova Cosmology Project, which is presently studying SNe Ia in galaxy clusters at very high z.

While the low- and high-redshift intervals are often targeted, the intermediate-redshift $(0.1 \lesssim z \lesssim 0.4)$ region is still an almost unexplored zone. We started a programme to have a well-covered sample of SNe Ia in that redshift range. In this paper, we present the spectroscopic results of the observations done in spring 2002, as part of the *International Time Programme* (*ITP*) project on supernovae for their physics and cosmology (PI: Ruiz-Lapuente).[8] These supernovae were identified using the 4.2 m William Herschel Telescope. We discuss where these supernovae belong in the empirical physical diagrams used to describe the supernova density profile and temperature. The results of the photometric follow-up and their cosmological implications will be presented in a forthcoming paper. There are prospects that Sloan Digital Sky Survey (SDSS-II; Sako et al. 2005) will provide a large sample of SNe Ia at those z, while the SNFactory (Aldering et al. 2004) will concentrate in supernovae at $z \sim 0.1$. At ENO, our own collaboration plans to move to very high z to carry out campaigns that will explore the physics of SNe Ia in detail at these high z in a similar way as done for the nearby sample. Physical properties of SNe Ia can be better studied within the intensive supernova campaigns by collecting a large database of spectra and photometry for each individual supernova. This task has been the aim of the RTN on Physics of Type Ia supernovae which compares each single SN Ia with model spectra to better understand SNe Ia explosions

---

(Hillebrandt et al. 2005). Detailed spectral evolution provides a complete probe of the SNe Ia ejecta: chemical composition, velocity, and other physical characteristics of the layers that successively become transparent.

At high z, the observing time per supernova has to be optimized. Long exposure times are needed to obtain good signal-to-noise ratio (S/N) spectra for the large number of candidates in the supernova searches. Limited telescope access prevents the program from having a complete sequence of spectra. However, as we will show here, one can go a step beyond what has been done up to now with high-z SN spectra and do a finer classification. In this intermediate-z campaign (see Ruiz-Lapuente 2006 for a review), we have shown how information similar to the one gathered in nearby SNe Ia can be gathered at all redshifts. This is a progress study of the possibilities offered by spectroscopy to better constrain the luminosity of intermediate- and high-z supernovae within the SN Ia family. The sample used here is limited, but the same analysis could be used in large samples collected by the various collaborations.

Spectral studies of intermediate-z supernovae have started to incorporate the study of expansion velocities of the material within the ejecta (Altavilla et al. 2005; Balastegui et al. 2005; Méndez et al. 2005; Balland et al. 2006). The intermediate-redshift spectra gathered here offer the possibility of investigating where the SNe Ia stand in terms of the distribution of chemical elements in velocity space and the temperature within the ejecta (Branch et al. 1993, 2006; Hatano et al. 2000; Benetti et al. 2004, 2005). This opens a new window to the inside of the supernova ejecta and allows testing for the existence of continuity in the temperature and spatial gradient characteristics of SNe Ia. Ultimately, these intermediate-redshift SNe Ia will help to fill the gap between the local and high-z SN samples, reducing the statistical uncertainties by means of an evenly sampled Hubble diagram. These supernovae are to be used for cosmology in conjunction with those gathered in other surveys.

The outline of this paper is as follows. In Section 2, we present the observations and the data reduction procedure, and in Section 3, the SN candidates' classification. In Section 4, we comment upon the results for individual objects and bring them into comparison with the nearby sample. Matches of the spectra to nearby SNe Ia are examined. In Section 5, the physical diagrams for intermediate-z SNe Ia are first built up in a way similar to what is done in nearby SNe Ia. The prospects of the use of these diagrams to reduce systematic uncertainties are shown. Further discussion is presented in Section 6. A brief summary of the run and conclusions are reported in Section 7.

2. OBSERVATIONS AND DATA REDUCTIONS

Spectra of the SN candidates were obtained using the 4.2 m William Herschel Telescope (WHT).[9] Observations were done using the spectrograph ISIS on 2002 June 10th and 11th (Table 1). A dichroic allowed simultaneous observations in the blue and red channels, which are optimized for their respective wavelength ranges (∼3000–6000 Å, ∼5000–10000 Å). In the blue, the R158B grating was used in conjunction with the EEV12 detector. In the red, we used the R158R grating + GG495 filter[10] and the MARCONI2 detector. In the red channel, fringing begins

---

[9] The WHT is operated by the Isaac Newton Group of Telescopes (ING), located at the Roque de Los Muchachos Observatory, La Palma, Spain.
[10] An order-separation filter designed to filter out second order blue from the first order red in usual applications, in the case of ISIS, where a dichroic splits the beam into red and blue channels, it helps define the "red" channel short wavelength.

Table 1
Journal of Spectroscopic Observations

| SN | Date | JD | Telescope | Exposure Time (s) | | Slit |
	(UT)	−2,400,000	Instrument	Blue Arm	Red Arm	(arcsec)
2002li	2002 Jun 10	52,436.6	WHT+ISIS	900	900	1.20
	2002 Jun 10	52,436.7	WHT+ISIS	900	900	1.20
	2002 Jun 10	52,436.7	WHT+ISIS	900	900	1.20
2002lj	2002 Jun 11	52,437.4	WHT+ISIS	900	900	1.20
	2002 Jun 11	52,437.4	WHT+ISIS	900	900	1.03
2002lp	2002 Jun 10	52,436.5	WHT+ISIS	900	900	1.20
	2002 Jun 10	52,436.5	WHT+ISIS	900	900	1.20
2002lq	2002 Jun 10	52,436.4	WHT+ISIS	900	900	1.20
	2002 Jun 10	52,436.5	WHT+ISIS	900	900	1.20
2002lr	2002 Jun 10	52,436.7	WHT+ISIS	900	900	1.20
	2002 Jun 10	52,436.7	WHT+ISIS	900	900	1.20
2002lk	2002 Jun 10	52,436.4	WHT+ISIS	300	300	1.20
	2002 Jun 10	52,436.4	WHT+ISIS	600	600	1.20
	2002 Jun 11	52,437.4	WHT+ISIS	600	600	1.20
2002ln	2002 Jun 10	52,436.6	WHT+ISIS	900	900	1.20
	2002 Jun 10	52,436.6	WHT+ISIS	900	900	1.20
2002lo	2002 Jun 11	52,437.6	WHT+ISIS	900	900	1.03
	2002 Jun 11	52,437.6	WHT+ISIS	900	900	1.03

at about 8000 Å and increases to ∼10% at 9000 Å. A long slit of 1″.2 was used in the first night, under good weather conditions, and a long slit of 1″.03 was adopted in the second night, under excellent weather conditions (except for SN 2002lk and one spectrum of SN 2002lj, which were observed at the beginning of the night with a 1″.2 slit). A journal of the spectral observations is given in Table 1.

Spectra were reduced following standard IRAF[11] procedures. All images were bias subtracted and then flat fielded using dome flats. The one-dimensional spectrum extractions were weighted by variance based on the data values and a Poisson/CCD model using the gain and read noise parameters. The background was interpolated by fitting two regions beside the spectra and then subtracted. Reference spectra of Cu–Ne–Ar lamps were used for the wavelength calibration. The results were checked measuring the position of bright [O I] sky lines at 5577 Å and 6300 Å and, when necessary, a rigid shift was applied to the spectrum to be consistent with these values. The spectra were flux calibrated using spectrophotometric standard stars observed at the start and at the end of each night. Correction for atmospheric absorption was applied to the red arm spectra. The blue and the red sections were joined in a single spectrum and multiple spectra of the same object were then combined in order to improve the S/N. Spectra with different exposure times were weighted accordingly.

3. CLASSIFICATION

3.1. Object, Redshift, and Phase Determination

Spectra can be inspected visually in order to give a rough classification of the SN candidate, where the main feature used to discriminate between Type Ia, Type II SNe, or "other" sources (typically quasi-stellar objects (QSOs) or active galactic nuclei (AGNs)) is the presence/absence of the strong Si II absorption at ∼6150 Å (rest frame) and the typical Si II ∼5400 Å (rest frame) "W" feature for SNe Ia. Type II SNe show the characteristic

---

[11] http://iraf.noao.edu/; IRAF is distributed by the National Optical Astronomy Observatories (NOAO), which are operated by the Association of Universities for Research in Astronomy (AURA), Inc., under cooperative agreement with the National Science Foundation.

Balmer series P Cygni profiles, most noticeably the Hα spectral feature. For a correct classification, one has to be aware of the possible confusion between SNe Ia and SNe Ic. This ambiguity increases its chances for cool SN Ia events when only one spectrum is available. As it will be shown in this paper, such ambiguity can be reduced if one uses the physical diagrams (expansion velocity and $\mathcal{R}(\text{Si II})$) in intermediate and high-z SNe Ia. For all those reasons and to find the best match in a library of SNe Ia, it is required to follow an automated procedure that will enable to quantify the difference of the spectra of the SNe Ia with those of an archive from a large sample of nearby SNe Ia at all phases.

The redshift of each supernova is obtained from the redshift of the host galaxy lines. In the case of no emission lines, it can be obtained by an algorithm that searches for the redshift that provides the best fit of the spectrum with a template. In our sample, the spectra were inspected looking for typical narrow galaxy lines: Balmer lines, [O II] λ3727, [O III] λ5007, [N II] λ6583, [S II] λ6716, 6731. The supernova spectra with the emission lines of the underlying host galaxy are shown in Figures 1–6 (top panels). The lines used for the redshift determination (when present) are shown. Uncertainties on the redshifts are of the order of 0.001 and they have been estimated by measuring the dispersion of the redshift determinations obtained from each identified galaxy line.

The following step was taken to refine the Type Ia SN classification by means of two different classification algorithms developed toward this aim. The first classification program transforms the spectra into the rest frame and compares it to a set of Type Ia supernovae spectral templates originally prepared by Nugent et al. (2002), and later adapted by Nobili et al. (2003). These spectral templates range from 19 days before maximum to 70 days after maximum, and the wavelength coverage is from 2500 Å to 25000 Å. Both the spectra and the templates are normalized in the wavelength range selected for the comparison, and then the spectra are again rescaled and shifted in the flux axis until the best match is found, see Figures 1–6 (middle panels). This procedure uses the whole spectrum and the result is not based on a few key features only.

In an interactive mode, the algorithm asks for a smoothing length and a sigma (σ) level to clean spikes in the observed spectrum. In this second mode, the procedure allows the user to specify the wavelength interval or to reject wavelength intervals of the comparison spectrum. This can be useful to reject a region of the spectrum highly contaminated with atmospheric absorption lines. Finally, the user can select the interval of redshifts and epochs used in the comparison.

Mathematically, the algorithm works by finding the minimum χ^2 of the observed spectrum compared with spectra of all the possible values of the epoch, j, and the redshift, z,

$$\chi_j^2(z) = \sum_{i=1}^{n} \frac{[f(\lambda_i) - F_j(\lambda_i, z)]^2}{\sigma_i^2}, \tag{1}$$

where n is the total number of data points of the observed SN spectrum, $f(\lambda_i)$ is the SN-normalized flux at wavelength λ_i, and $F_j(\lambda_i, z)$ is the template-normalized flux at wavelength λ_i, epoch j, and redshift z. The algorithm delivers rest-frame epoch, flux scale, and redshift as parameters. If the redshift is known from the narrow galaxy lines, the algorithm takes it as given and the redshift is not used in the minimization.

Once the first classification is obtained based on templates, a second analysis is done using an algorithm that compares
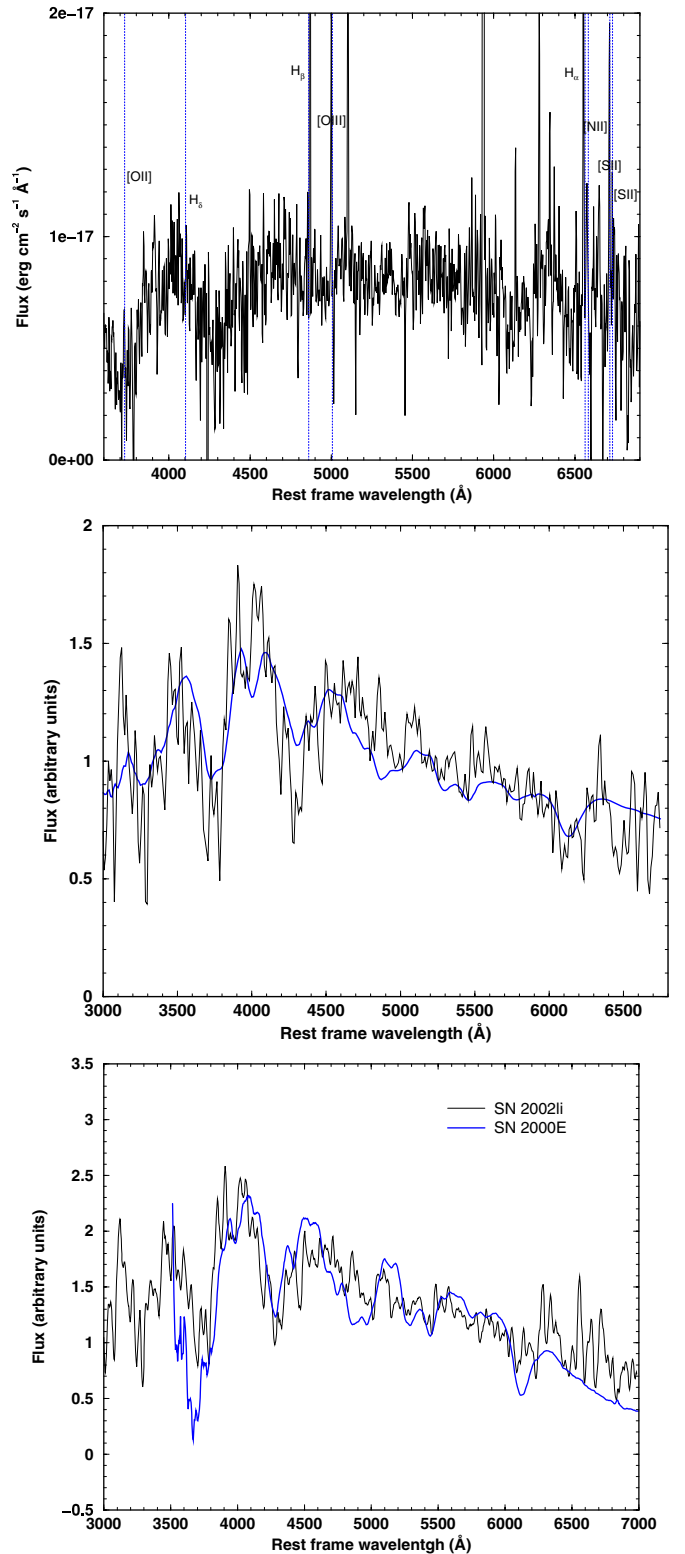

Figure 1. Top: spectrum of SN 2002li, including galaxy lines for the redshift determination. Middle: template fitting of SN 2002li spectrum. Template epoch is 2 days before maximum. SN 2002li spectrum has been dereddened and smoothed. Bottom: comparison of SN 2002li smoothed spectrum with that of SN 2000E 4 days before maximum. Both SN 2002li and SN 2000E spectra have been dereddened and smoothed.

(A color version of this figure is available in the online journal.)

the SNe Ia with those of the Padova SN Catalogue and other spectra available in the literature (we also made use of the
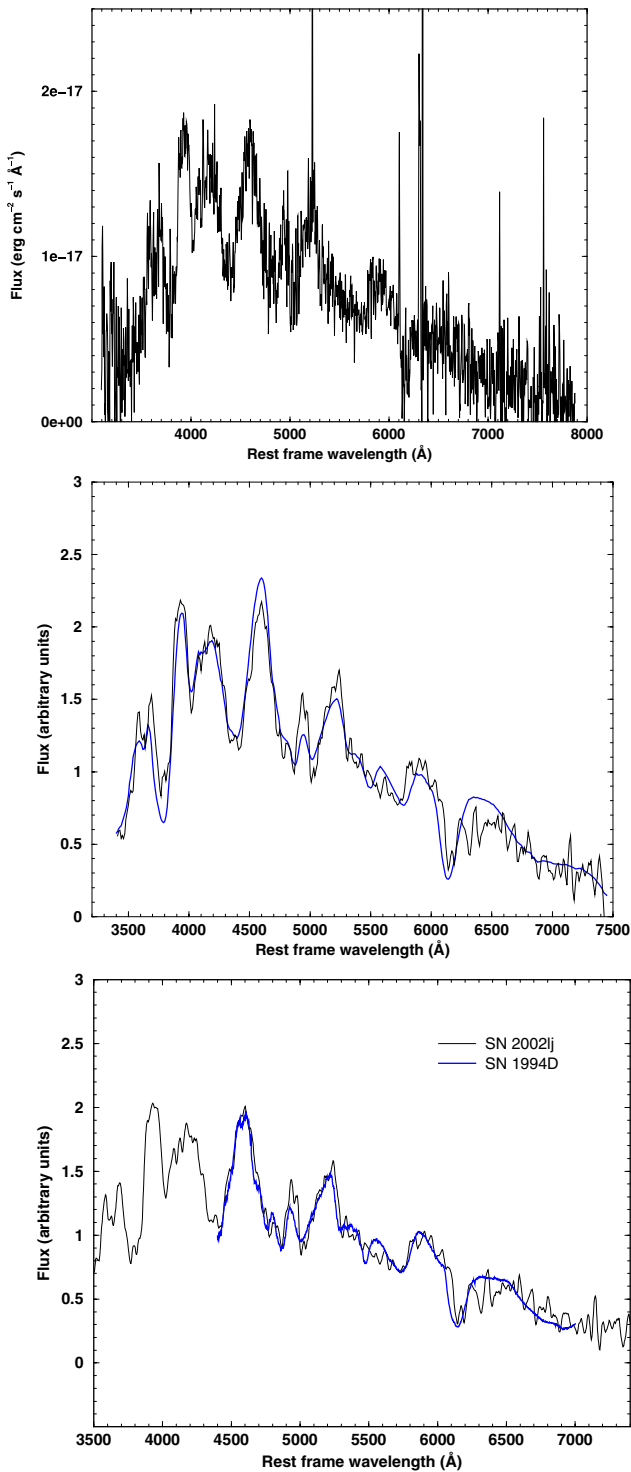
Figure 2. Top: Spectrum of SN 2002lj. No galaxy lines have been found. Redshift determined from supernovae features. Middle: Template fitting of SN 2002lj smoothed spectrum. Template epoch is 7 days past maximum. Bottom: Comparison of SN 2002lj spectrum with that of SN 1994D 7 days past maximum. Both spectra have been smoothed.

(A color version of this figure is available in the online journal.)

Figure 3. Top: spectrum of SN 2002lp, including galaxy lines for the redshift determination. Middle: template fitting of SN 2002lp spectrum. Template epoch is 3 days past maximum. SN 2002lp spectrum has been smoothed and dereddened. Bottom: comparison of SN 2002lp spectrum with that of SN 1989B at maximum. SN 2002lp spectrum has been dereddened. Both spectra have been smoothed.

(A color version of this figure is available in the online journal.)

SUSPECT database[12]). This allows us to find a real template which best fits the SN Ia (Figures 1–5, lower panel). The two algorithms *Genspecphase* and *Genspecsubtype* were developed for this programme and can be used in campaigns at all redshifts.
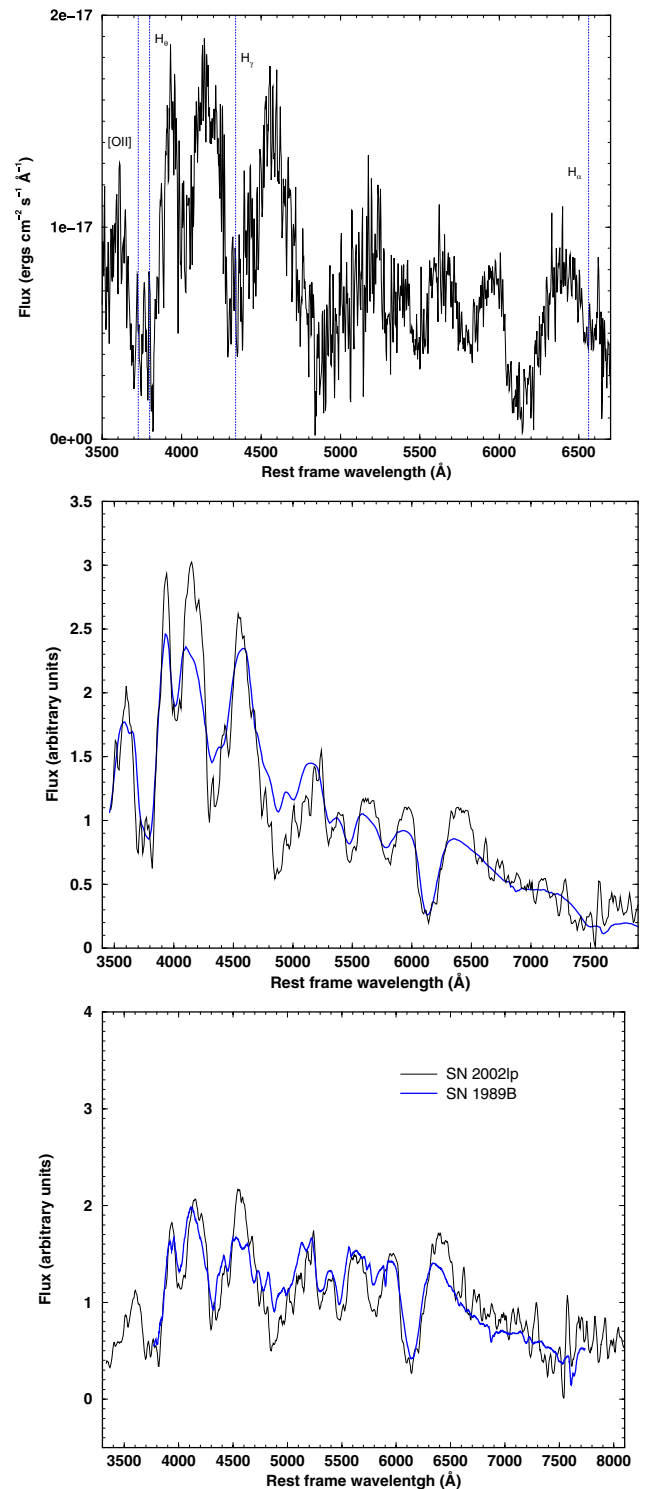
Results with the redshift z and phase determination can be seen in Table 2.

We estimated the spectral epoch and its uncertainty by comparing the phases obtained matching the spectra with the synthetic and real templates. We assumed a minimum error of
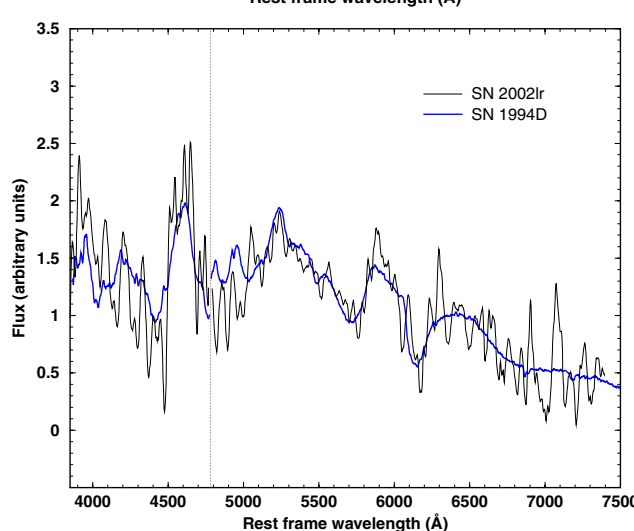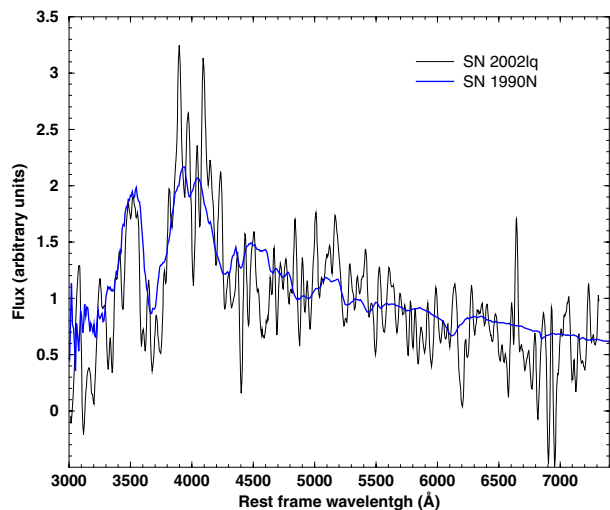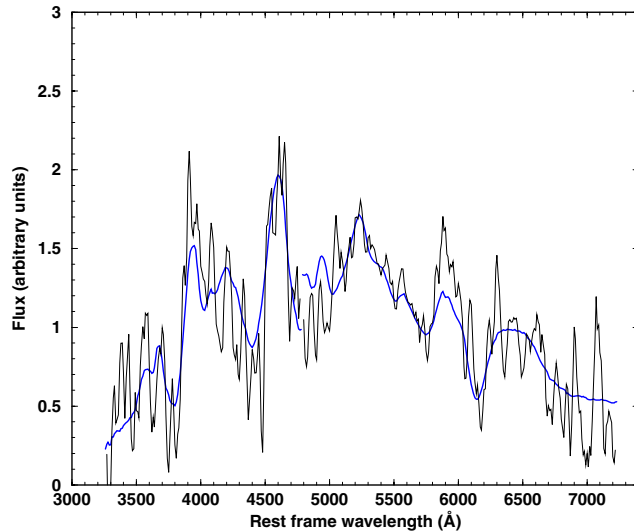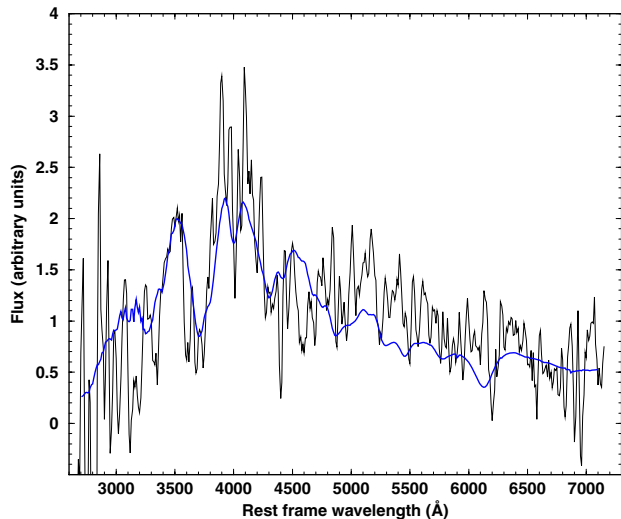

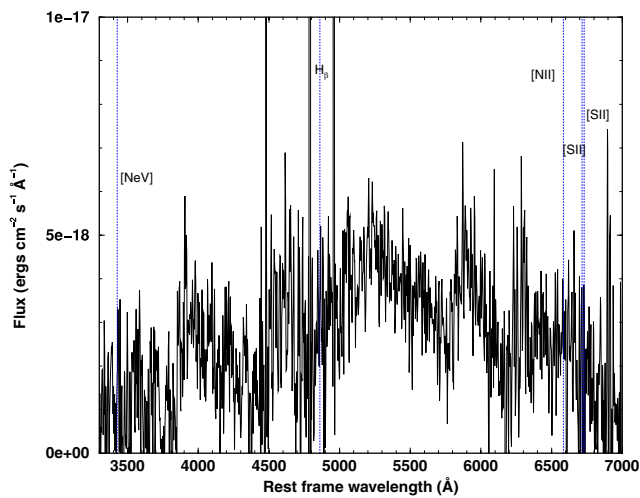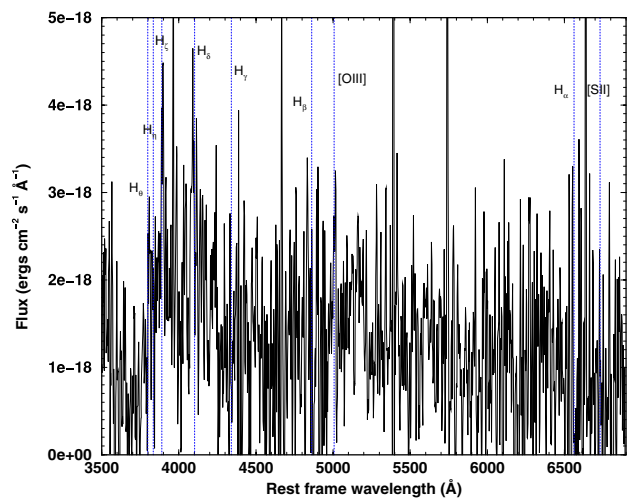[12] http://bruford.nhn.ou.edu/~suspect/index1.html

Figure 4. Top: spectrum of SN 2002lq, including galaxy lines for the redshift determination. Middle: template fitting of SN 2002lq spectrum. Template epoch is 7 days before maximum. SN 2002lq spectrum has been smoothed and dereddened. Bottom: comparison of SN 2002lq spectrum with that of SN 1990N 7 days before maximum. SN 2002lq spectrum has been smoothed and dereddened.

(A color version of this figure is available in the online journal.)

Figure 5. Top: spectrum of SN 2002lr, including galaxy lines for the redshift determination. Middle: template fitting of SN 2002lr smoothed spectrum. Template epoch is 10 days past maximum. Bottom: comparison of SN 2002lr spectrum with that of SN 1994D 10 days past maximum. Both spectra have been smoothed.

(A color version of this figure is available in the online journal.)

±2 days (see also Riess et al. 1997). The comparison of the spectral phase τ_{spec} with the phases τ_{pho} determined from the photometric data (see Table 2) shows that the spectral epochs

are correct within a few days, with a scatter of $\sigma = 3.5$ days (Figure 7). This value is consistent with the adopted spectroscopic phase error bars.
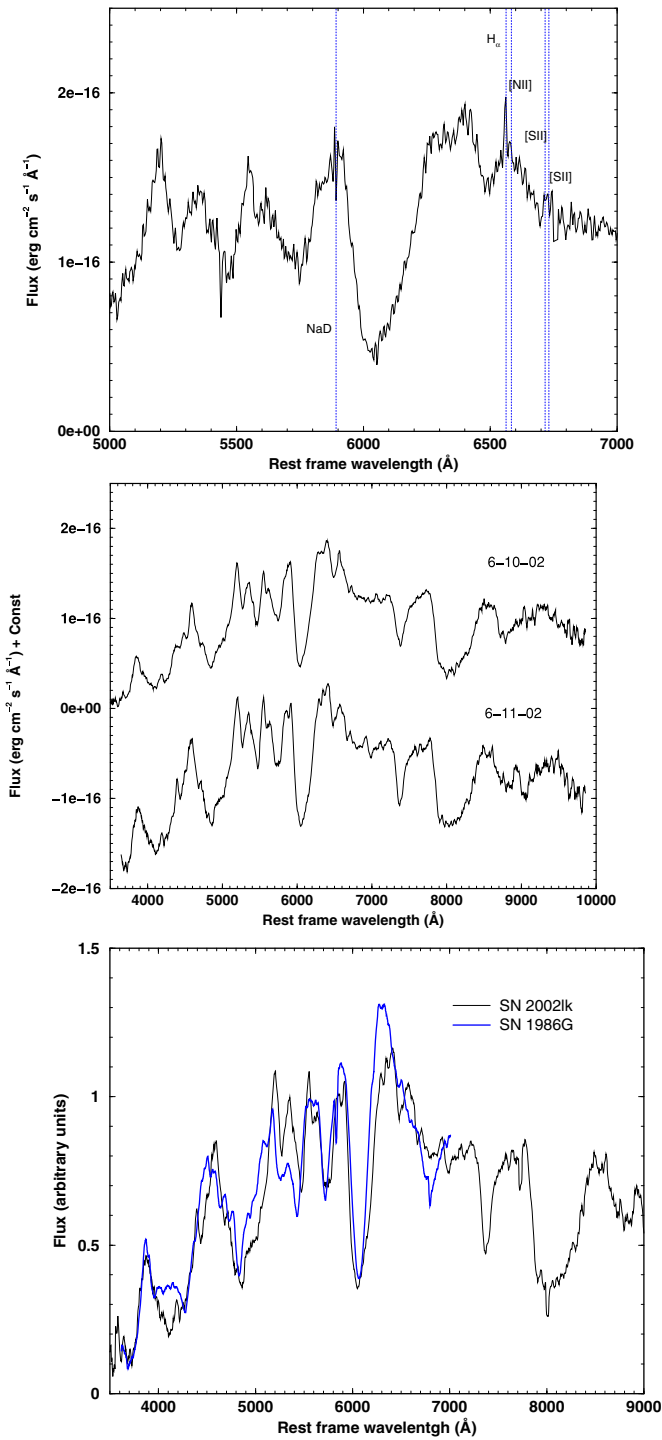
Figure 6. Top: spectrum of SN 2002lk on June 10, including galaxy lines for the redshift determination. Middle: spectra of SN 2002lk on June 10 and June 11 (-2×10^{-16} erg cm^{-2} s^{-1} Å^{-1}). Bottom: comparison of SN 2002lk spectrum on June 11 with that of SN 1986G 2 days before maximum. SN 1986G spectrum has been smoothed.

(A color version of this figure is available in the online journal.)

SN 2002lk presented an interesting test for classification. It was an intrinsically red (cool) SN Ia and in addition to that, it was highly reddened. A rough approach might have mistaken it for a SN Ic at another phase. We included a number of intrinsically red (cool) SNe Ia in our database as well as Type Ic supernovae to increase the quality of the classification. Consistency is found between the color light curves and the spectral classification.
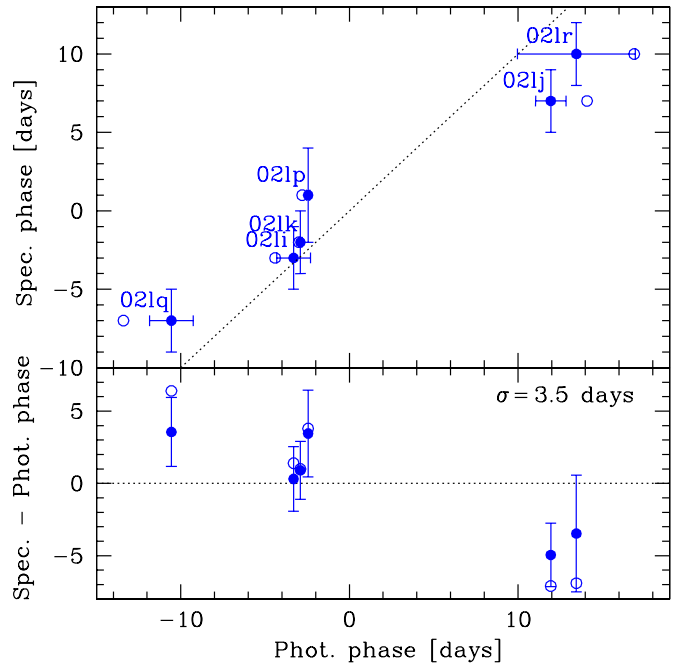

Figure 7. Comparison of the spectrum epochs as determined from the spectrum fits (τ_{spec}) and the light-curve fits (τ_{pho}). Filled dots: τ_{pho} corrected for time dilation; empty dots: τ_{pho} not corrected for time dilation. Epochs are relative to the B band maximum. The dispersion σ is relative to the corrected points. The dotted line corresponds to $\tau_{spec} = \tau_{pho}$.

(A color version of this figure is available in the online journal.)

Observed and template spectra have been smoothed and tilted with an absorption amount derived empirically within the classifying procedure. This "reddening factor" may not be totally due to absorption, as it is also intended to correct for light losses due to observations with the slit out of the parallactic angle and/or to take into account different colors between targets and templates, and/or to take into account reddened templates. In some cases, the spectral templates have been slightly red- or blueshifted to account for the small differences in the expansion velocities between the template and the observed SNe.

The peculiar Type Ia SN 2002lk and Type II SNe have been compared with real templates only (Figures 6, 8, and 9).

Table 3 summarizes the results of the classification of the host galaxies of all SN candidates.

3.2. Host Galaxy Morphology

Host galaxy morphology identification is usually accomplished by exploiting good imaging and spectra (Sullivan et al. 2003). In our sample, the visual identification of the host galaxy morphology is feasible for two objects only: SN 2002lq and SN 2002lk. The latter is a Type Ia SN similar to the underluminous SN 1986G, which exploded in a spiral galaxy (for a discussion on the host galaxies of SNe, see Howell 2001). The host galaxy of SN 2002lk has been classified as spiral since its ellipticity, larger than 7, is not consistent with an elliptical galaxy and, although it is observed almost edge on, the existence of some structure, as a dust lane, can be detected. An image of the galaxy about one year after explosion reveals also the bulge of the galaxy.

The rest of the galaxy images do not give hints of the galaxy morphology, being compatible with both elliptical and spiral galaxies (in the latter case the possible spiral structure is
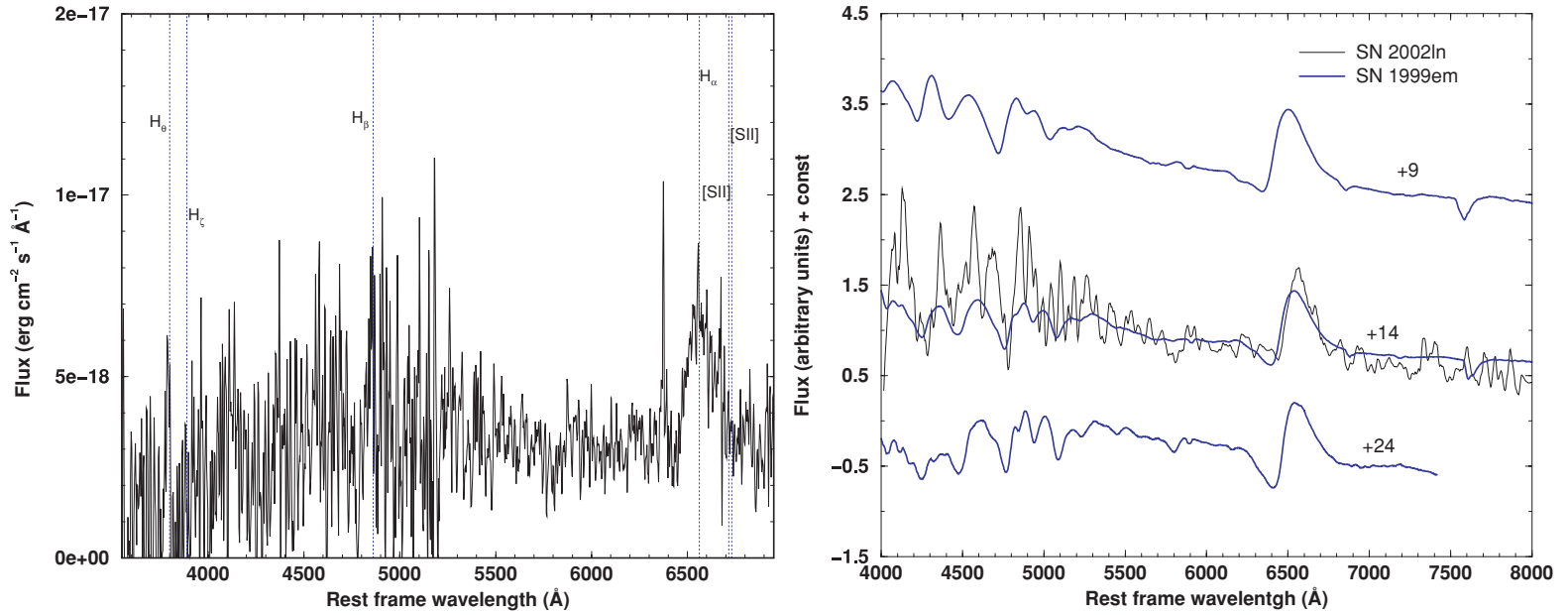
Figure 8. Left panel: spectrum of the Type II supernova SN 2002ln, including galaxy lines for the redshift determination. Right panel: comparison of SN 2002ln spectrum with that of SN 1999em about 9, 14, and 24 since B maximum. Both SN 2002ln and SN 1999em spectra have been smoothed.

(A color version of this figure is available in the online journal.)

Table 2
Summary of Observations

Object Name	Date (UT)	R.A.(2000.0) (hh mm ss)	δ(2000.0) (° ′ ″)	Redshift	Object Type	Notes τ_{spec}^a	τ_{pho}^b	Number^c
SN 2002li	2002 Jun 10	15:59:03.08	+54:18:16.0	0.329	SN Ia	-3 ± 2	-3.31 ± 1.0	5
SN 2002lj	2002 Jun 11	16:19:19.65	+53:09:54.2	0.180	SN Ia	$+7 \pm 2$	$+11.95 \pm 0.9$	8
SN 2002lp	2002 Jun 10	16:40:11.45	+42:28:30.2	0.144	SN Ia	$+1 \pm 3$	-2.45 ± 0.1	8
SN 2002lq	2002 Jun 10	16:40:28.83	+41:14:09.1	0.269	SN Ia	-7 ± 2	-10.56 ± 1.3	6
SN 2002lr	2002 Jun 10	22:33:12.59	+01:05:56.7	0.255	SN Ia	$+10 \pm 2$	$+13.47 \pm 3.5$	5
SN 2002lk	2002 Jun 11	16:06:55.92	+55:28:18.2	0.033	SN Ia.	-2 ± 2	-2.90 ± 0.1	14
SN 2002ln	2002 Jun 10	16:39:24.93	+41:47:29.0	0.138	SN II	$\sim +14$	...	...
SN 2002lo	2002 Jun 11	16:39:56.42	+42:19:20.5	0.136	SN II	$\sim +35$	...	...

Notes.
^{a} Spectral epoch from the spectroscopic analysis.
^{b} Spectral epoch (rest-frame) from the photometric analysis.
^{c} Number of epochs of photometry.

unresolved). Since we have no spectra of the host galaxies alone, the identifications given are made exclusively on the basis of the galaxy lines contaminating the SNe spectra (Kennicutt 1992). Thus, we will only distinguish between spheroidal galaxies (ellipticals and lenticulars) and spiral galaxies.

SN 2002li and SN 2002lq have host galaxies that are classified as spiral galaxies, since they have a good number of lines from the Balmer series. The host galaxy morphology of the host of SN 2002lq can be also inferred from visual inspection, while the structure of the host galaxy of SN 2002li is not as clear as for the previous case.

SN 2002lj lacks galaxy lines. Without any clear Balmer emission line, we have classified it as a spheroidal galaxy.

SN 2002lp has Hα, Hγ, and Hθ in emission, but very faint. Its host galaxy is possibly spiral. The spectrum of SN 2002lr also presents narrow emission lines.

The Type II SNe, SN 2002ln, and SN 2002lo, show narrow emission lines of the Balmer series. Their host galaxies have been classified as spirals (Table 3).

4. SPECTROSCOPIC CLASSIFICATION

4.1. Type Ia Supernovae

SN 2002li: This is the farthest supernova discovered in this search ($z = 0.329$). Figure 1 (bottom panel) shows the comparison with SN 2000E (Valentini et al. 2003), an SN which is almost identical spectroscopically to SN 1990N, i.e., a typical Type Ia SN. Both the comparisons with SN 2000E and Nobili's spectral templates (Figure 1, middle panel) suggest that the SN 2002li phase corresponds to a few days before maximum.

The blueshifted H and K lines at 3950 Å indicate that the expansion velocity of Ca II in SN 2002li is $\sim$17,200 km s^{-1}, lower than for SN 2000E ($\sim$21,000 km s^{-1}). The S/N does not allow a reliable determination of the expansion velocity of Si II at $\sim$6150 Å. Photometric data suggest that SN 2002li is a slow decliner object ($\Delta m_{15}(B) \sim 0.79 \pm 0.22$), but being spectroscopically normal. In the local sample, slow decliners are often normal spectroscopically (Hamuy et al. 2002).
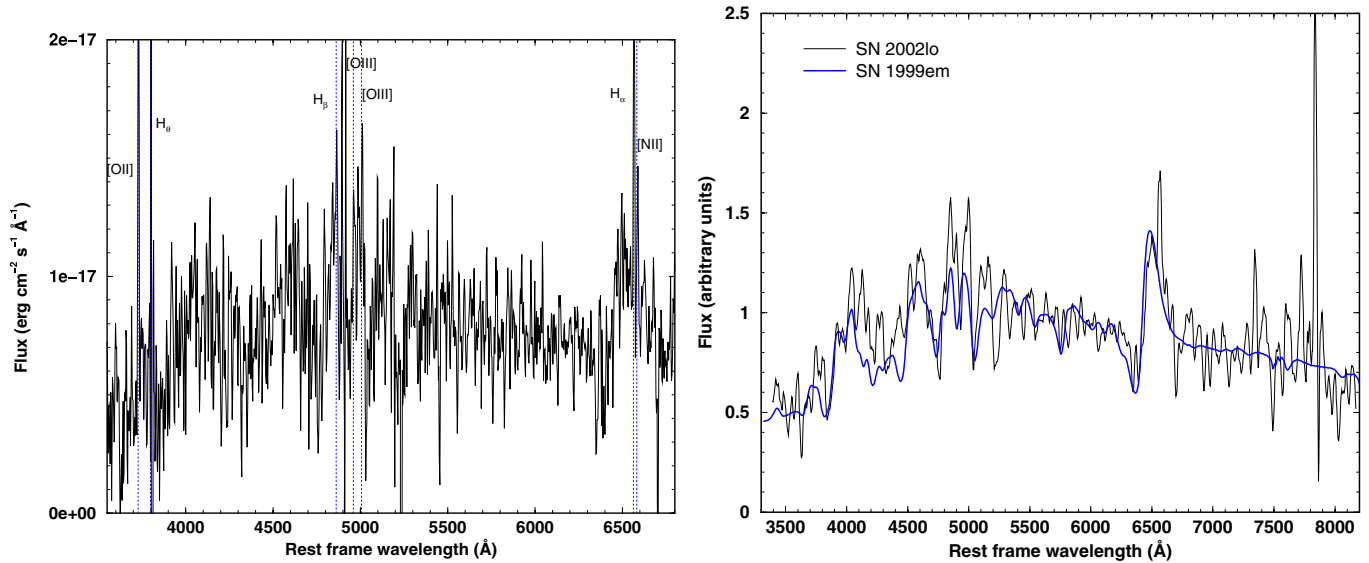
Figure 9. Left panel: spectrum of the Type II supernova SN 2002lo, including galaxy lines for the redshift determination. Right panel: comparison of SN 2002lo spectrum with that of SN 1999em ∼35 days since *B* maximum. Both SN 2002lo and SN 1999em spectra have been smoothed.
(A color version of this figure is available in the online journal.)

Table 3
Host Galaxy Morphology

SN Ia	z	Galaxy Type	Offset		Identified Lines	Imaging[a]
2002li	0.329	Spiral	0″.1 W	0″.2 S	H_α, H_β, H_δ, [S II], [N II], [O III], [O II]	y
2002lj	0.180	Spheroidal	0″.2 W	…	…	n
2002lp	0.144	Spiral?	0″.2 E	2″.0 N	H_α, H_γ, H_θ, [O II]	n
2002lq	0.269	Spiral	4″.5 E	0″.7 S	H_α, H_β, H_γ, H_δ, H_ζ, H_η, H_θ, [S II], [O III]	y
2002lr	0.255	Spiral?	3″.0 S	…	H_β, [S II], [N II], [Ne V]	n
2002lk	0.033	Spiral (Sb)	0″.7 W	0″.2 N	H_α, [S II], [N II], Na D	y
2002ln	0.138	Spiral	1″.1 W	8″.3 S	H_α, H_β, H_ζ, H_θ, [S II]	n
2002lo	0.136	Spiral	0″.6 E	1″.3 S	H_α, H_β, H_θ, [N II], [O III], [O II]	y

Note.
[a] Host galaxy morphology can be inferred (y) or not (n) from visual inspection.

SN 2002lj: The redshift of SN 2002lj has been derived from SNe features due to the absence of measurable galaxy emission lines. Both the matches with a real SN (SN 1994D; Patat et al. 1996; Figure 2, bottom panel) and a template spectrum (Figure 2, middle panel) suggest that the observed epoch for SN 2002lj is about a week past maximum. Since SNe Ia still show S II features between 5500 Å and 5700 Å as late as 7 days after maximum, the absence of these features in the SN 2002lj spectrum suggests a phase out to roughly a week past maximum. The redshift was found by comparison with the template SN features, thus most of them have the same expansion velocity, except Si II at 6355 Å, whose expansion velocity for SN 2002lj is lower (∼8900 km s^{-1}) than that measured for SN 1994D (∼9800 km s^{-1}).

SN 2002lp: The comparison of the spectra of SN 2002lp with that of 1989B at maximum (Barbon et al. 1990; Wells et al. 1994) shows that they are quite similar events (Figure 3, bottom panel). The match with a template at day 3 after maximum (Figure 3, middle panel) confirms that the spectrum of SN 2002lp was taken close to maximum. The expansion velocity measured from the Si II unresolved doublet 6355 Å (∼10,400 km s^{-1}) is almost coincident with that measured for SN 1989B (∼10,000 km s^{-1}). The absorption dip at ∼5800 Å, identified as Si II 5972 Å, is stronger than that in SN 1989B. This is quantified by the $\mathcal{R}$(Si II) parameter or ratio of the two Si II absorptions dips, i.e., the one

at ∼5800 Å and the one at ∼ 6150 Å (Nugent et al. 1995). In SN 2002lp, $\mathcal{R}$(Si II) is 0.50 ± 0.05 and in SN 1989B it is 0.29 ± 0.05 for the same period.

The match with a template at day 3 after maximum confirms that the spectrum of SN 2002lp was taken near maximum. The expansion velocities measured from the Si II unresolved doublet (6355 Å) and Ca II lines (3950 Å) (∼10,400 km s^{-1}, ∼13,800 km s^{-1}, respectively) are almost coincident with the those measured for SN 1981B (∼10,400 km s^{-1}, ∼14,000 km s^{-1}). While the velocities for SN 2002lp are in the range of those found in SN1981B, the absorption dip at ∼5800 Å, identified as Si II 5972 Å, is stronger than that in SN 1981B. In SN 1981B, $\mathcal{R}$(Si II) is 0.16 ± 0.05 near maximum, a value which is typical for normal SNe Ia. The spectral comparison with the complete SNe Ia library finds that SN 1989B is the best match for this supernova (Figure 3, bottom panel).

SN 2002lq: The comparison with SN 1990N, a typical SN Ia with good spectral coverage (Leibundgut et al. 1991), suggests that SN 2002lq is a Type Ia SN observed about one week before maximum (Figure 4, bottom panel). This is true despite the fact that the Si II (6355 Å) feature, if existent, is very faint. Matching synthetic templates gives a phase of 7 days before maximum for this supernova (Figure 4, middle panel). The only clearly visible feature in this low S/N spectrum is Ca II line at 3950 Å, and its expansion velocity (∼18,900 km s^{-1}), measured with large

uncertainty, appears somewhat lower than that of SN 1990N ($\sim$21,000 km s^{-1}).

SN 2002lr: This Type Ia supernova was observed about 10 days after maximum, as derived from fitting the templates and fitting to real SNe Ia (Figure 5, middle and bottom panels). SN 2002lr spectrum is similar to that of SN 1994D (Patat et al. 1996) 10 days past maximum. The expansion velocity derived from Si II (6355 Å; $\sim$8600 km s^{-1}) is similar to that derived for SN 1994D ($\sim$9500 km s^{-1}). The expansion velocity measured from the Ca II line at 3950 Å is $\sim$12,800 km s^{-1} but it is not possible to compare this value with the corresponding one in SN 1994D because the limited spectral range of the template does not allow the measurement of the Ca II line.

SN 2002lk: For SN 2002lk two different spectra are available since it was observed in two consecutive nights (Figure 6). The strong similarities between the spectra of SN 2002lk and SN 1986G (Phillips et al. 1987; Padova SN Catalogue) suggest that SN 2002lk is an SN 1986G-like event observed a few days before maximum. Due to the supernova's peculiarities, a comparison with Nobili's spectral templates is not appropriate. In Figure 6, the spectra of SN 1986G have been shifted in wavelength in order to match better that of SN 2002lk. This small shift takes into account the different expansion velocities of the two objects. For SN 2002lk the velocity determined from the Si II line at 6355 Å is $\sim$14,500 km s^{-1}, while for SN 1986G it is $\sim$10,800 km s^{-1}. The significant difference between the two values might be attributable to different explosion energies. SN 2002lk is characterized by a higher expansion velocity, slower decline rate in the B light curve ($\Delta m_{15}(B) \sim 1.23 \pm 0.02$), and similar $\mathcal{R}$(Si II) values with respect to SN 1986G. Thus, SN 2002lk, in its turn, can be considered a less extreme object with respect to SN 1986G ($\Delta m_{15}(B)$ is 1.69 $\pm$0.05 for SN 1986G), suggesting a continuous transition from object to object. We note that similar high expansion velocity was found for SN 1998de, a 1991bg-like SN (Modjaz et al. 2001), whose expansion velocity (6 days before maximum) derived from the Si II (6355 Å) minimum was 13,300 km s^{-1} (Garnavich et al. 1998).

As far as reddening is concerned, the detection of the Na I D ($\lambda\lambda$5890, 5896 Å) allows us to estimate the host galaxy component of the color excess $E(B-V)$. The host galaxy is a spiral galaxy, and the supernova is highly reddened by the galaxy dust lane. By means of an empirical relation between the equivalent width (EW) of the Na I D lines and $E(B-V)$ (Barbon et al. 1990; Richmond et al. 1994; Turatto et al. 2003) we estimated $0.15 \leqslant E(B-V) \leqslant 0.5$ ($0.46 \leqslant A_V \leqslant 1.55$), where the two values correspond to two different slopes of the relation found by Turatto et al. (2003). The color excess $E(B-V) = 0.56 \pm 0.04$ derived from the photometric data is consistent with the higher value obtained from the spectroscopic analysis. The Galactic component of the absorption is quite negligible: $A_V = 0.025$ (Schlegel et al. 1998). The spectrum of SN2002lk has a very flat bottom Ca II and Si II absorption troughs. The shape of these absorption features suggests that this is a highly asymmetric supernova, like SN 2004dt (Altavilla et al. 2007).

4.2. Type II Supernovae

SN 2002ln and SN 2002lo: Both Type II SNe are matched with SN 1999em as template, a normal Type II plateau (Elmhamdi et al. 2003). The phase is not so well defined for SN 2002ln since the blue part of the spectrum has a low S/N. A comparison of SN 2002ln with SN 1999em at 9, 14 (Hamuy et al. 2001),
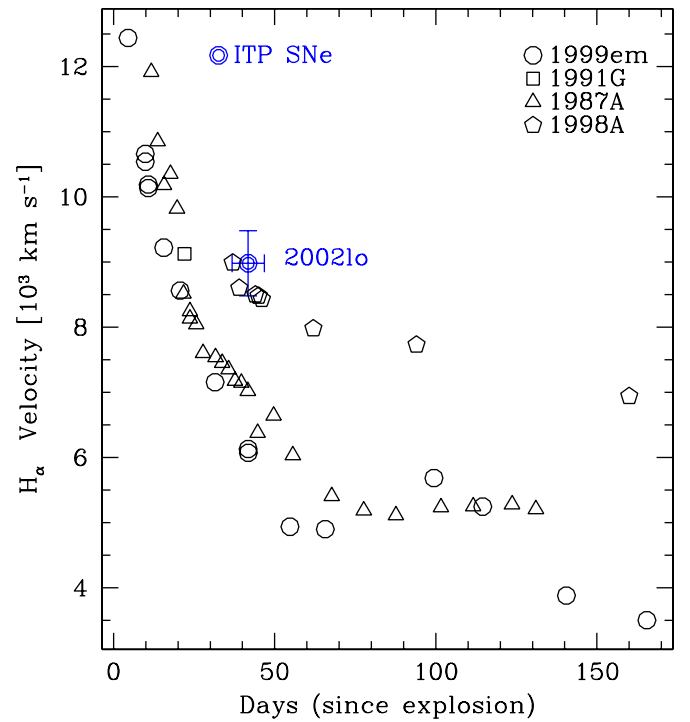

Figure 10. Expansion velocity for Hα (6562.8 Å) as deduced from its minimum, in SN 2002lo, compared with those of SN 1999em (Elmhamdi et al. 2003), 1991G (Blanton et al. 1995), 1987A (Phillips et al. 1989), and 1998A (Pastorello et al. 2005).

(A color version of this figure is available in the online journal.)

and 24 (Leonard et al. 2002) days since B maximum, shown in Figure 8, suggests a phase of about two weeks. The Hα minimum is not measurable, and the peak of the P Cygni profile, in principle expected to be at null velocity, is slower in SN 2002ln ($\sim$220 km s^{-1} for SN 2002ln, $\sim$2500 km s^{-1} for SN 1999em).

A comparison with SN 1999em at $\sim$35 days since B maximum (Leonard et al. 2002) shows that SN 2002lo is about one month old (Figure 9). The expansion velocity measured from the Hα minimum in SN 2002lo ($\sim$8980 km s^{-1}) is slightly higher than that measured for SN 1999em ($\sim$6100 km s^{-1}; Figure 10), while the peak of the P Cygni profile is faster for SN 2002lo ($\sim$1500 km s^{-1}) with respect to SN 1999em ($\sim$950 km s^{-1}). Uncertainties for our measurements are of the order of 500 km s^{-1}. However, Type II plateau SNe, and Type II SNe in general, are a very heterogeneous class, showing a wide range in the photometric and spectroscopic properties (Patat et al. 1994; Filippenko 1997).

5. $\mathcal{R}$(Si II) PARAMETER AND EXPANSION VELOCITIES

Several diagrams can help us to learn about these intermediate-z SNe Ia as stellar explosions and allow a comparison with the nearby sample. Expansion velocities for Ca II (3950 Å) and Si II (6355 Å) lines have been measured from the blueshift of the lines, as in the local sample. The ratio of the two Si II lines, i.e., Si II (6355 Å) and Si II (5890 Å) defines the $\mathcal{R}$(Si II) parameter as introduced by Nugent et al. (1995). We measure the $\mathcal{R}$(Si II) parameter following the same procedure as these authors: drawing segments between adjacent continuum points of the absorption lines and measuring the difference in flux between the higher excitation transition of the two (those transitions are the 4P–5S and the 4S–4P). If the photosphere has
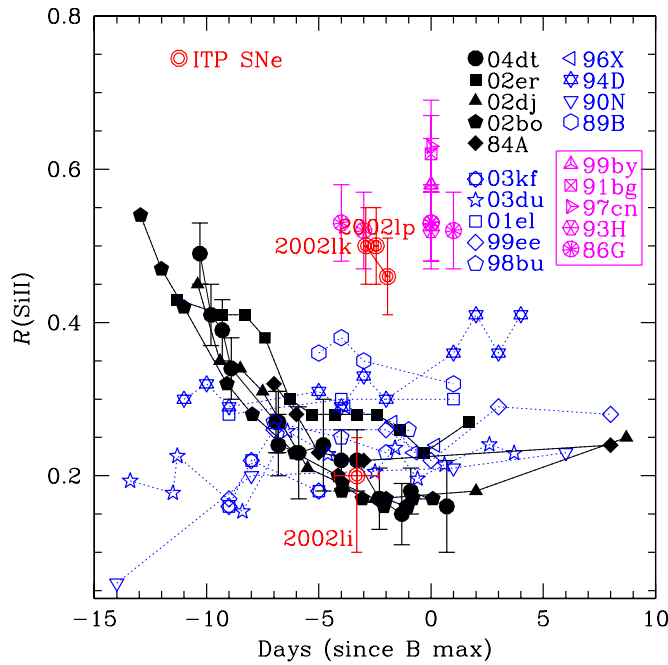
Figure 11. $\mathcal{R}(\mathrm{Si\ II})$ parameter for SN 2002lk, SN 2002lp, and SN 2002li, and for a sample of nearby SNe shown as comparison. Filled symbols refer to high velocity gradient SNe, open symbols to low velocity gradient SNe as defined in Benetti et al. (2005). FAINT SNe, listed in the box, are also shown.

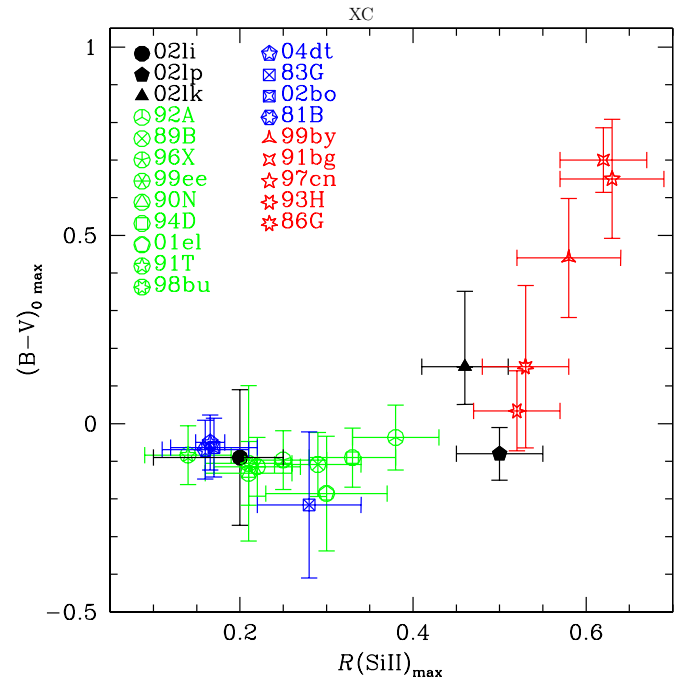(A color version of this figure is available in the online journal.)

Figure 12. $\mathcal{R}(\mathrm{Si\ II})$ parameter and intrinsic $(B - V)$.

(A color version of this figure is available in the online journal.)

a higher effective temperature T_{eff}, one would expect that the 5800 Å trough would increase toward higher T_{eff} and a lower value of $\mathcal{R}(\mathrm{Si\ II})$. The behavior in SNe Ia is, however, twofold at very early phases (Figure 11). In one group, $\mathcal{R}(\mathrm{Si\ II})$ is seen to decrease significantly from the premaximum hotter phase toward the maximum. This is found in SNe Ia like SN2002bo and SN2004dt which present significant 5800 Å troughs compared to the one at 6150 Å in this premaximum phase, while in another group it is the opposite: $\mathcal{R}(\mathrm{Si\ II})$ increases from the premaximum hotter phase toward the maximum phase in SNe Ia like SN 1990N or stays constant like in SN2003du. Such diversity of behaviors could be linked to the presence of Fe and Co in the outer layers. According to Nugent et al (1995), the Si II lines interact with line blanketing from Fe III and Co III at premaximum when the temperature is high and Fe and Co are substantially present in the outer layers. This effect washes out the 5800 Å trough. The decrease of $\mathcal{R}(\mathrm{Si\ II})$ at premaximum in SN 1990N could be due to Fe and Co in the outer layers, as this supernova showed these elements in the premaximum spectra. The supernovae which behave like SN 2004dt and SN2002bo do not have substantial Fe in the outer layers (Altavilla et al. 2007). In SN 2002bo, intermediate-mass elements were most abundant in the outer layers (Stehle et al. 2004). The high $\mathcal{R}(\mathrm{Si\ II})$ is consistent with the expectation of minor line blanketing by Fe III and Co III.

While we have discussed this ratio at premaximum, which could be an indicator of the physics of the outer layers, we find that at maximum the time evolution in $\mathcal{R}(\mathrm{Si\ II})$ is quite flat, and one can define a parameter $\mathcal{R}(\mathrm{Si\ II})_{\mathrm{max}}$. The blanketing by Fe III and Co III at this epoch is likely negligible, as such high ionization stages are not found with the lower temperatures at maximum. At that epoch $\mathcal{R}(\mathrm{Si\ II})_{\mathrm{max}}$ correlates well with absolute magnitude: the more luminous the SNe Ia the lower the $\mathcal{R}(\mathrm{Si\ II})_{\mathrm{max}}$ and the fainter the SNe Ia the higher the $\mathcal{R}(\mathrm{Si\ II})_{\mathrm{max}}$. A recent investigation of the tight correlation between $\mathcal{R}(\mathrm{Si\ II})_{\mathrm{max}}$

and luminosity points to an ionization balance as the cause of the correlation (Hachinger et al. 2008). According to these authors, in less luminous objects, Si II λ 5972 would be stronger because of the rapidly increasing Si II/Si III ratio in cooler supernovae. We have investigated using our sample in Figure 12 the $\mathcal{R}(\mathrm{Si\ II})_{\mathrm{max}}$ ratio versus intrinsic color of the supernova, which should also correlate with absolute magnitude. We find that the bluer SNe Ia have smaller $\mathcal{R}(\mathrm{Si\ II})_{\mathrm{max}}$. The intermediate-$z$ SNe Ia in this figure follow the trend defined by nearby SNe Ia. For consistency of our comparison between the intermediate-z sample and the nearby sample, the $\mathcal{R}(\mathrm{Si\ II})$ ratio has been measured in a similar way. In both cases, we follow Nugent et al. (1995) in defining the continuum and the minimum of the absorption troughs. The $E(B - V)$ in the nearby sample is measured using the Lira–Phillips relation (Lira 1995; Phillips et al. 1999) for the tail of the $B−V$ color, which allows the determination of the excess $E(B - V)$ by comparison of the tail from 30 to 60 days after maximum with the tail of unreddened SNe Ia (the tail in that epoch shows very low dispersion). In the intermediate-z SNe Ia, the same has been done when observations after maximum were available and, in the absence of these, we use the color curve for the stretch of the SNe Ia (Nobili et al. 2003). This is being done to get the correct $B−V$ color in the presence of extinction. The $E(B - V)$ values derived from the color light curves for the sample of intermediate SNe Ia are very small except for SN 2002lk which is derived to be $E(B - V) = 0.56 \pm 0.04$ and for SN 2002lp which is derived to be 0.15 ± 0.05. For the rest, $E(B - V)$ is consistent with zero, the upper limit being 0.01.

We have been able to measure $\mathcal{R}(\mathrm{Si\ II})_{\mathrm{max}}$ for all the SNe Ia found at maximum. In our sample, spectra of two of the SNe Ia were taken one week or more after maximum. At that phase, the Si II 5800 Å trough is replaced by iron lines and $\mathcal{R}(\mathrm{Si\ II})_{\mathrm{max}}$ cannot be measured at that late epoch. In the premaximum SN 2002lq the S/N level does not allow us to measure this ratio. It has been possible to obtain a good measurement of this ratio for SN 2002lk and SN 2002lp and it was measured with larger error bars for SN2002li (see Table 4). Figure 11 shows the ratio

Table 4
Expansion Velocities for Ca II (3950 Å) and Si II (6355 Å) Lines and $\mathcal{R}$(Si II) Ratio

Object	Phase[a]	Exp. Velocity	Exp. Velocity	$\mathcal{R}$(Si II)
Name	Since B Max.	Ca II (km s^{-1})	Si II (km s^{-1})	
SN 2002li	-3.31 ± 1.0	$17,200 \pm 500$	. . .	$0.2^{+0.05}_{-0.10}$
SN 2002lj	11.95 ± 0.9	$12,300 \pm 300$	$8,900 \pm 300$	. . .
SN 2002lp	-2.45 ± 0.1	$13,800 \pm 900$	$10,400 \pm 400$	0.50 ± 0.05
SN 2002lq	-10.56 ± 1.3	$18,900 \pm 1400$	. . .	. . .
SN 2002lr	13.47 ± 3.5	$12,800 \pm 300$	$8,600 \pm 400$	. . .
SN 2002lk	-2.90 ± 0.1	. . .	$14,500 \pm 500$	0.50 ± 0.05
SN 2002lk	-1.94 ± 0.1	. . .	$13,850 \pm 500$	0.46 ± 0.05

Note.
[a] From the light curve fitting.

$\mathcal{R}$(Si II) of the depth of the Si II 5972 and Si II 6355 Å absorption troughs (see Nugent et al. 1995; Benetti et al. 2005). SN2002lp and SN2002lk show remarkably high $\mathcal{R}$(Si II) values a few days before maximum, consistent with what is found for red, faint SN Ia. SN 2002li has values for $\mathcal{R}$(Si II)$_{max}$ consistent with what is found from SNe Ia of the same brightness in the nearby sample.

6. DISCUSSION

The spring run of the ITP 2002 on SNe Ia for Cosmology and Physics gave six Type Ia SNe, two Type II SNe, seven quasars, and two Seyfert galaxies. The redshift range of all the sample is $0.033 \leqslant z \leqslant 2.89$ while the SN redshift range is $0.033 \leqslant z \leqslant 0.329$. As expected in a magnitude-limited survey, the peak in the redshift distribution of Type II SNe is closer than the peak in redshift of Type Ia SNe. On the other hand, QSOs are observed up to very high redshift (Figure 13).

Our sample allowed a careful inspection of SNe Ia. We have made a comparison of the kinematic and temperature observables in these intermediate-z SNe Ia with those of the nearby sample. Some SNe Ia were intrinsically red, and as in the nearby sample, showed a large ($\sim$0.5 near maximum) $\mathcal{R}$(Si II)$_{max}$ ratio. Other SNe Ia were bluer with $(B - V)_0 < 0$ near maximum light. Those showed a small $\mathcal{R}$(Si II)$_{max}$ ratio ($\sim$0–0.2 near maximum), as in the nearby sample. Among the intrinsically red SNe Ia, also called cool SNe Ia, we find SN 2002lk and SN 2002lp. Those cool SNe Ia are similar to SN 1986G but with less extreme characteristics (higher expansion velocity, slower decline rate of the B light curve). SN 2002lp is a cool SN Ia similar to SN 1989B. It is an SN Ia with characteristics intermediate to SN1989B and SN1986G. It has a deeper Si II $\sim$5800 Å line and larger $\mathcal{R}$(Si II)$_{max}$ than SN1989B. Both SN 2002lk and SN 2002lp show a similar $\mathcal{R}$(Si II) value ($\sim$0.5). SN 2002lk and SN 2002lp have some other common characteristics: they have the largest $\Delta m_{15}(B)$, they are the closest, and the intrinsically faintest Type Ia SNe in the sample. Such a trend is in accordance with that could happen under the expectations of cosmological selection effects.

Peculiar events such as SN 2000cx and SN 2002cx are not represented in this small sample of intermediate-z SNe Ia. While in a larger sample of SNe Ia at intermediate z, events belonging to those hot subclasses could be found, it has not been the case in the present sample. We have only found cool or normal SNe Ia.

The interesting aspect shown here is that the intrinsic faintness of the SNe Ia is not only revealed by a low stretch factor, i.e., high $\Delta m_{15}(B)$, but also from the large $\mathcal{R}$(Si II) values (Nugent et al. 1995; Benetti et al. 2005) which correlate with intrinsic color
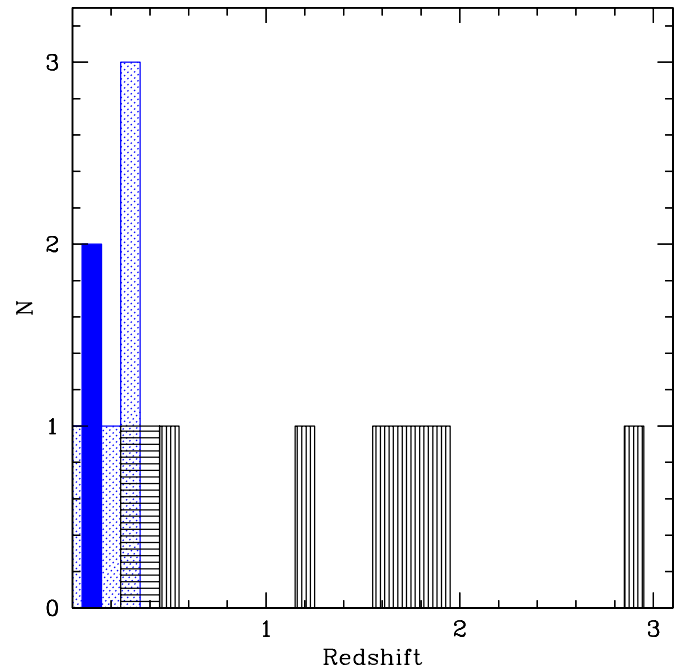

Figure 13. Redshift distribution of the observed objects. Filled histogram: Type II SNe; dotted histogram: Type Ia SNe; horizontal line histogram: Seyfert galaxies; vertical line histogram: QSOs; redshift bin: 0.1.
(A color version of this figure is available in the online journal.)

(see Figure 12). This fact opens new avenues for a better control over reddening in SNe Ia samples gathered in cosmological surveys. The present small sample study give prospects for a better control of color in large samples. Figures 11 and 12 could be supplemented with new measurements to assess the usefulness of this approach.

The expansion velocities measured for all the SNe Ia in this intermediate-z sample are consistent with the values measured for nearby SNe (Figure 14).

Most Type Ia SNe in this sample occurred in spiral galaxies (Table 3). The Type II SNe observed exploded in spiral galaxies as well. The fraction of Type Ia SNe that exploded in spirals can be as high as 83% if we take into account the uncertain classification of the host galaxy of SN 2002lp and SN 2002lr. Despite being limited by the small statistics and by the rough discrimination between spheroidal and spiral galaxies, our result is consistent with the ones derived in a similar redshift range by Valenti et al. (2005) and Balland et al. (2006) (94% and 83% of Type Ia host galaxies are respectively classified as spirals). These values can be compared to the results derived by Sullivan et al. (2003, and references therein) at low redshift ($z < 0.01$, 88%) and high redshift ($0.19 \leqslant z \leqslant 0.83$, 71%).

The comparison between the spectral phase determined from the spectral analysis and from the photometric analysis shows a good agreement between the two estimates ($\sigma = 3.5$ days). The agreement gets significantly worse if the time dilation correction $(1 + z)$ is not taken into account in the light-curve fitting ($\sigma = 5.6$ days). The time dilation effect is non-negligible at this z range and measurable in those spectra as in high-z SNe Ia.

7. CONCLUSIONS

In this paper, we present SNe Ia in the poorly studied area of intermediate z, in the redshift range $0.033 \leqslant z \leqslant 0.329$. The comparison of intermediate-z SN spectra with high S/N spectra
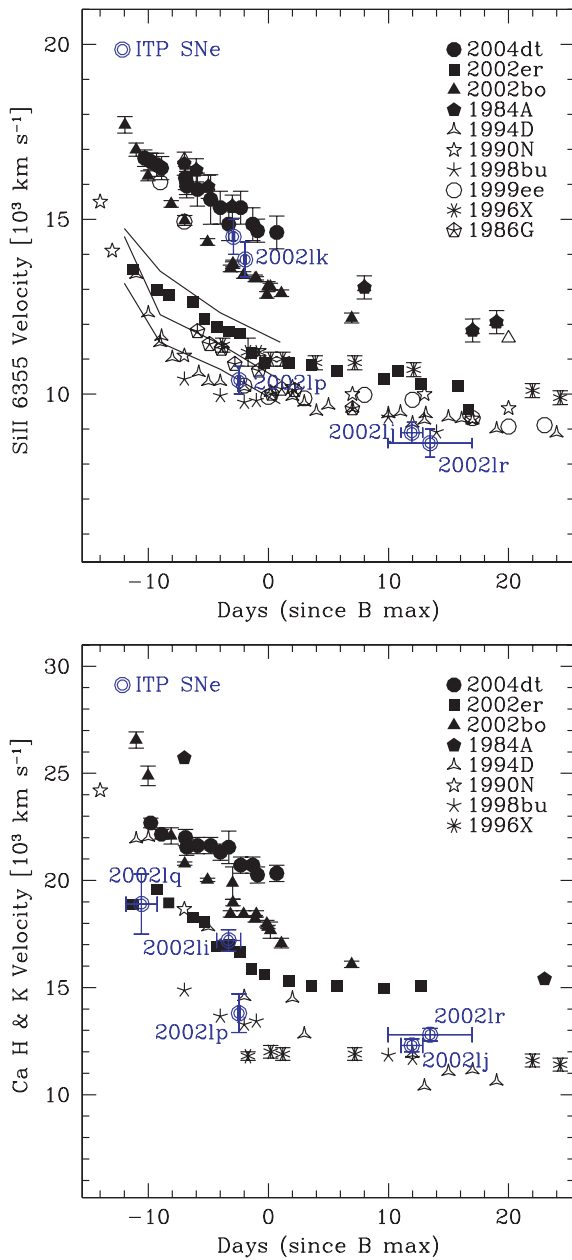
Figure 14. Expansion velocities for Si II (6355 Å; upper panel) and Ca II (3950 Å; lower panel) as deduced from their minima, compared with those of other SNe. The Si II evolution expected for different metallicities (solid line, top: ×10 solar metallicity; middle: ×1; bottom: ×0.1) is also shown (Lentz et al. 2000). The phase has been determined from the light-curve fitting.
(A color version of this figure is available in the online journal.)

of nearby SNe has not revealed significant differences in the spectral features and kinematics. In particular, for all the Type Ia SNe of our sample, including a peculiar one, it has always been possible to find a nearby Type Ia SN counterpart, and the expansion velocities derived from the Si II and Ca II lines are within the range observed for nearby Type Ia SNe. The spectral concordance seems to correspond as well with trends seen in the peak color and decline of the light curve. The comparison between the epochs determined for each spectrum from the spectral analysis and the photometric epochs derived from fits of the light curves shows values in agreement within a few days.

The main conclusion of this research is that the $\mathcal{R}$(Si II) parameter is useful for investigating the physics of SNe Ia
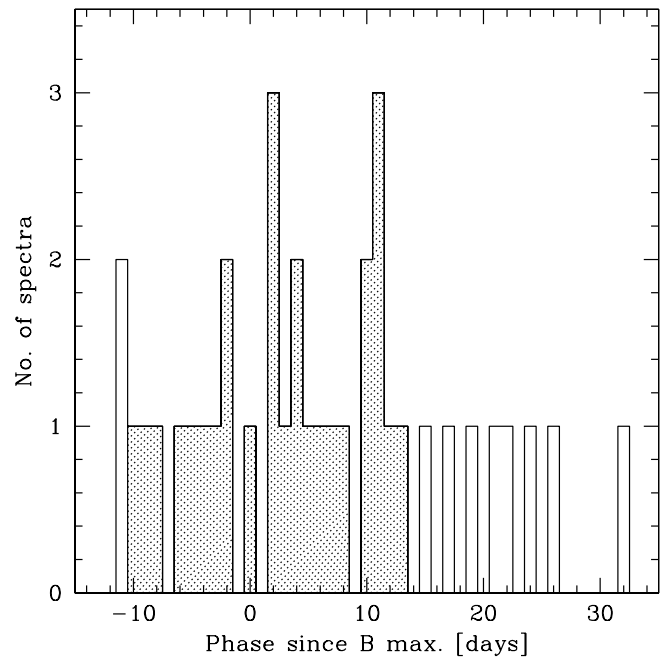

Figure 15. Phase distribution of the normal SN Ia templates listed in Table 5 (limited to 35 days since B maximum). The dotted area shows the phase range of our SN Ia sample.

explosions at high redshift and serves as meaningful comparison with the nearby SNe Ia sample. It can help to place individual supernova in the sequence of bright–faint SNe Ia (sequence correlated with slow–fast decline and with bluer–redder at maximum). It provides a control over reddening that can be very useful to reduce systematic uncertainties. While the category of large $\mathcal{R}$(Si II)$_{max}$ contains faint and intrinsically redder SNe Ia, in the side of low $\mathcal{R}$(Si II)$_{max}$ one finds the intrinsically bluer SNe Ia. We have found that intermediate and nearby SNe Ia follow a similar $\mathcal{R}$(Si II)$_{max}$–$(B-V)_0$ behavior and the intermediate-z SNe Ia occupy the same space in the evolution of $\mathcal{R}$(Si II) along time than nearby ones. Similar results are found for the expansion velocity, though a larger sample of SNe Ia at all epochs needs to be investigated.

While the behavior of $\mathcal{R}$(Si II) with epoch can be linked to luminosity and color properties, there is no trend correlating $\mathcal{R}$(Si II)$_{max}$ with the expansion velocities of Si II or Ca II. In the side of large $\mathcal{R}$(Si II)$_{max}$ one can have SNe Ia with a large Si II velocity or with a lower one. Therefore, velocity of the intermediate-mass elements is not a tracer of the luminosity according to the present sample. We also have some doubts about the correlation of asymmetries in the ejecta with overall luminosity of the SN Ia. SN2002lk is a faint and red SN Ia which shows high asymmetries in the Si and Ca lines, while SN 2004dt, a normally luminous SN Ia, has those asymmetries as well.

The $\mathcal{R}$(Si II) at epochs well before maximum is an observable quantity of great value and accessible to high-z SNe Ia searches. While $\mathcal{R}$(Si II)$_{max}$ correlates well with intrinsic color, $\mathcal{R}$(Si II)$_{premax}$ can identify the composition of the outer layers of the SNe Ia observed in cosmological searches. Thus, with the same spectra obtained in the discovery runs one can investigate the nature of those explosions.

This research was carried through the International Time Programme *Omega and Lambda from Supernovae and the*

Table 5
SN Ia Templates

SN	Type	N. Spectra	Time Coverage[a]	$\Delta m_{15}(B)$	Reference(s)	
1986G	Ia pec.	39	−4..+324	1.69(0.05)	Phillips et al. (1987)	Pd-As Cat.-SUSPECT
1989B	Ia	8	0..+52	1.28(0.05)	Barbon et al. (1990)	Pd-As Cat.-SUSPECT
1990N	Ia	6	+2..+333	1.05(0.05)	Leibundgut et al. (1991)	Pd-As Cat.-SUSPECT
. . .	. . .	. . .	. . .	. . .	Mazzali et al. (1993)	. . .
1994D	Ia	31	−11..+106	1.31(0.05)	Patat et al. (1996)	Pd-As Cat.-SUSPECT
1999em	II P	40	−1..+515	. . .	Hamuy et al. (2001)	Pd-As Cat.-SUSPECT
. . .	. . .	. . .	. . .	. . .	Leonard et al. (2002)	. . .
2000E	Ia	7	−6..+124	0.94(0.05)	Valentini et al. (2003)	Pd-As Cat.-SUSPECT

Note.
[a] Since B maximum.

APPENDIX

SPECTRAL TEMPLATES

The spectral analysis has been performed using both synthetic and real spectra. In particular we used 90 synthetic SN Ia spectra by Nobili et al. (2003), based on Nugent's spectral templates (Nugent et al. 2002; http://supernova.lbl.gov/~nugent/nugent_templates.html). Phases range from −19 to +70 days since B maximum, with 1 day step. Wavelength coverage is from 2500 Å to 25000 Å, but in our analysis the useful range is limited up to ∼10000 Å.

We also made use of real spectral templates, mainly collected from the Padova-Asiago SN Catalogue (Pd-As Cat.) (http://web.pd.astro.it/supern/snean.txt; Barbon et al. 1990) and SUSPECT database (http://bruford.nhn.ou.edu/~suspect/), spanning a wide range in the decline rates ($\Delta m_{15}(B)$) of the corresponding B band light curves. In particular, we used the spectra listed in Table 5. Table 5 shows the spectra available of the comparison SNe Ia that best match our intermediate-z ones, while Figure 15 shows their phase distribution.

REFERENCES

Aldering, G., et al. 2004, Proc. SPIE, 4836, 61
Altavilla, G., et al. 2005, in ASP Conf. Ser. 342, 1604–2004: Supernovae as Cosmological Lighthouses, ed. M. Turatto, S. Benetti, L. Zampieri, & W. Shea (San Francisco, CA: ASP), 486
Altavilla, G., et al. 2007, A&A, 475, 585
Astier, P., et al. (The SNLS Collaboration) 2006, A&A, 447, 31A
Balastegui, A., et al. 2005, in ASP Conf. Ser. 342, 1604–2004: Supernovae as Cosmological Lighthouses, ed. M. Turatto, S. Benetti, L. Zampieri, & W. Shea (San Francisco, CA: ASP), 490
Balland, C., et al. 2006, A&A, 445, 387
Barbon, R., Benetti, S., Cappellaro, E., Rosino, L., & Turatto, M. 1990, A&A, 237, 79
Barris, B. J., et al. 2004, ApJ, 602, 571
Benetti, S., et al. 2004, MNRAS, 348, 261
Benetti, S., et al. 2005, ApJ, 623, 1011
Blanton, E. L., Schmidt, B. P., Kirshner, R. P., Ford, C. H., Chromey, F. R., & Herbst, W. 1995, AJ, 110, 2868
Branch, D., Fisher, A., & Nugent, P. 1993, AJ, 106, 2383
Branch, D., et al. 2006, PASP, 118, 560B
Clocchiatti, A., et al. 2006, ApJ, 642, 1
Elmhamdi, A., et al. 2003, MNRAS, 338, 939
Filippenko, A. V. 1997, ARA&A, 35, 309
Garnavich, P., Jha, S., & Kirshner, R. 1998, IAU Circ. 6980
Hachinger, S., Mazzali, P., Tanaka, M., Hillebrandt, W., & Benetti, S. 2008, MNRAS, 389, 1087
Hamuy, M., Phillips, M. M., Suntzeff, N. B., Nicholas, B., Schommer, R. A., Maza, J., & Aviles, R. 1996, AJ, 112, 2398
Hamuy, M., et al. 2001, ApJ, 558, 615
Hamuy, M., et al. 2002, AJ, 124, 417
Hatano, K., Branch, D., Lentz, E. J., Baron, E., Filippenko, A. V., & Garnavich, P. M. 2000, ApJ, 543, 49
Hillebrandt, W., et al. 2005, http://www.mpa-garching.mpg.de/ rtn
Hook, I. M., et al. 2005, AJ, 130, 2788
Howell, D. A. 2001, ApJ, 554, 193
Kennicutt, R. C. 1992, ApJSS, 79, 255
Knop, R. A., et al. 2003, ApJ, 598, 102
Kowalski, M., et al. 2008, ApJ, 686, 1087
Krisciunas, K., et al. 2005, AJ, 130, 2453
Leibundgut, B., Kirshner, R. P., Filippenko, A. V., Shields, J. C., Foltz, C. B., Phillips, M. M., & Sonneborn, G. 1991, ApJ, 371, 23
Lentz, E. J., Baron, E., Branch, D., Hauschildt, P. H., & Nugent, P. E. 2000, ApJ, 530, 966
Leonard, D. C., et al. 2002, PASP, 114, 35
Lira, P. 1995, Master thesis, Univ. Chile
Mazzali, P. A., Lucy, L. B., Danziger, I. J., Gouiffes, C., Cappellaro, E., & Turatto, M. 1993, A&A, 269, 423
Méndez, J., et al. 2005, in ASP Conf. Ser. 342, 1604–2004: Supernovae as Cosmological Lighthouses, ed. M. Turatto, S. Benetti, L. Zampieri, & W. Shea (San Francisco, CA: ASP), 488
Modjaz, M., Li, W., Filippenko, A. V., King, J. Y., Leonard, D. C., Matheson, T., Treffers, R. R., & Riess, A. G. 2001, PASP, 113, 308
Nobili, S., Goobar, A., Knop, R., & Nugent, P. 2003, A&A, 404, 901
Nugent, P., Kim, A., & Perlmutter, S. 2002, PASP, 114, 803
Nugent, P., Phillips, M., Baron, E., Branch, D., & Hauschildt, P. 1995, ApJ, 455, 147
Pastorello, A., et al. 2005, MNRAS, 360, 950
Patat, F., Barbon, R., Cappellaro, E., & Turatto, M. 1994, A&A, 282, 731
Patat, F., Benetti, S., Cappellaro, E., Danziger, I. J., della Valle, M., Mazzali, P. A., & Turatto, M. 1996, MNRAS, 278, 111
Perlmutter, S., et al. 1999, ApJ, 517, 565
Phillips, M. M., Heathcote, S. R., Hamuy, M., & Navarrete, M. 1989, AJ, 95, 1087
Phillips, M. M., et al. 1987, PASP, 99, 592
Phillips, M. M., et al. 1999, ApJ, 118, 1766
Richmond, M. W., Treffers, R. R., Filippenko, A. V., Paik, Y., Leibundgut, B., Schulman, E., & Cox, C. V. 1994, AJ, 107, 1022
Riess, A. G., et al. 1997, ApJ, 114, 722
Riess, A. G., et al. 1998, AJ, 116, 1009
Riess, A. G., et al. 2004, ApJ, 607, 665
Riess, A. G., et al. 2007, ApJ, 659, 98

Ruiz-Lapuente, P. 2006, in Proc. of Bernard's Cosmic Stories (http://www.astro.rug.nl/~bernard60)

Sako, M., et al. 2005, AAS, 207, 15002

Schlegel, D. J., Finkbeiner, D. P., & Davis, M. 1998, ApJ, 500, 525

Stehle, M., Mazzali, P. A., Benetti, S., & Hillebrandt, W. 2004, MNRAS, 360, 1231

Sullivan, M., et al. 2003, MNRAS, 340, 1057

Tonry, J. L., et al. 2003, ApJ, 594, 1

Turatto, M., Benetti, S., & Cappellaro, E. 2003, in Proc. ESO/MPA/MPE Workshop: From Twilight to Highlight—The Physics of Supernovae, ed. B. Leibundgut & W. Hillebrandt (Berlin: Springer), 200

Valentini, G., et al. 2003, ApJ, 595, 779

Valenti, S., et al. 2005, in ASP Conf. Ser. 342, 1604–2004: Supernovae as Cosmological Lighthouses, ed. M. Turatto, S. Benetti, L. Zampieri, & W. Shea (San Francisco, CA: ASP), 505

Wells, L. A., et al. 1994, AJ, 108, 2233

Wood-Vasey, W. M., et al. 2007, ApJ, 666, 694